European Polymer Journal 76 (2016) 28–39

Contents lists available at ScienceDirect

European Polymer Journal

journal homepage: www.elsevier.com/locate/europolj

Recycled HDPE reinforced with sol–gel silica modified wood sawdust

Witold Brostow *, Tea Datashvili, Peter Jiang, Harrison Miller

Laboratory of Advanced Polymers & Optimized Materials (LAPOM), Department of Materials Science and Engineering and Department of Physics, University of North Texas, 3940 North Elm Street, Denton, TX 76207, USA[1]

ARTICLE INFO

Article history:
Received 30 August 2015
Received in revised form 4 January 2016
Accepted 6 January 2016
Available online 7 January 2016

Keywords:
Polymer + wood composites
Wood sawdust modification
Thermal expansivity
Dynamic mechanical analysis
Brittleness
Scratch resistance

ABSTRACT

The goal of the work was improvement of mechanical and tribological properties of high density polyethylene (HDPE) while finding use for wood sawdust (wood flour). Two chemical modification methods have been used for wood sawdust treatment to improve compatibility between the HDPE matrix and wood sawdust. Traditional silane coupling was used as a first approach to modify the sawdust by 3-methacryloxypropyl-trimethoxysilane (3MPS) and thereby forming C—O—Si bonds. As a second method, we decided to combine sol–gel process with 3MPS treatment to form Si—O—Si and C—O—Si linkages. Silica nanoparticles are filling wood fiber cells and silica rods formation is seen; as a result, thermal expansivity decreases. As expected, the enthalpy of fusion and the degree of crystallinity go down with increasing filler concentration. Tensile modulus goes up as result of filler loading while the tensile strain at break goes down. As the result, brittleness *B* goes up somewhat, but overall the values of *B* are quite low. With one exception, residual depth in scratch resistance testing decreases as a consequence of introduction of the fillers. Addition of unmodified wood results in increasing dynamic friction, chemical modification of wood particles results in lowering friction. Combination of focused ion beam milling with scanning electron microscopy shows clearly positive effects of modification on adhesion between the phases.

1. Introduction

One-half of all industrial materials used in the United States are wood-based [1]. Wood is the basic material for furniture, interior decorating, and construction industries. The increasing demand for good-quality wood has resulted in over-logging of extensive non-renewable hardwood timber in many tropical rain forests. There is an urgent need to find suitable substitutes for good quality wood [2]. Polymer + wood composites (PWCs) have been in existence for a long time; however, the increasing cost of virgin plastics and the limited availability of appropriate wood fiber restrict their rapid development. Recycling and reuse of wood fiber, thermoplastics, and their virgin composite products have great potential. In recent years, about 190 million metric tons of municipal solid waste have been generated in the United States [3–8]. Waste wood, waste paper, and waste plastics are major components of municipal solid waste (MSW); this waste offers great opportunities for making recycled ingredients into wood fiber + plastic composites.

* Corresponding author.
E-mail addresses: wkbrostow@gmail.com (W. Brostow), tea_datashvili@yahoo.com (T. Datashvili).
[1] http://www.unt.edu/LAPOM/.

http://dx.doi.org/10.1016/j.eurpolymj.2016.01.015
0014-3057/

Using sawdust in this fashion provides an additional use for recycled wood fibers—and thus further reduces waste in landfills. The wood flour is clean, consistent, inexpensive, free flowing, and readily available as a waste byproduct from secondary manufacturing operations. However, there is a problem with using wood sawdust as filler for thermoplastics; the thermoplastic interacts poorly with the wood cell wall surface, which lowers the overall strength of the composites [9–17]. The thermoplastic matrix holds the wood, but since poor adhesion exists between wood and polymer, stresses do *not* transfer across the interface between the wood and polymer matrix. The higher surface energy of the cellulose fibers does not correspond to a lower surface energy of the polymer. This gives rise to a distinct interface between the thermoplastic and reinforcing cellulose fibers. Literature tells us clearly how important interfaces are for composite properties [18–22].

Since polymers are often hydrophobic while wood and wood products are hydrophilic [23], modification of the filler, or the matrix, or both, helps [24]. The methods for surface modification of fillers can be physical or chemical. Frequently used approaches include bleaching, acetylation, and alkali treatments. The main chemical method used in the surface modification of natural wood fibers is chemical coupling [12,16,25–27]. The most commonly used coupling agents are maleated polyolefins [11,25]. There have also been studies on other coupling agents such as isocyanates [28] and silanes [25–27]. Other chemical methods involve changing the surface tension to improve impregnation of the fibers by a matrix [16,29]. However, in the past, neither chemical nor physical methods have significantly improved the interfacial adhesion and the thermal–mechanical properties of PWCs.

2. Scope and objectives

In this situation, we have used post-consumer high density polyethylene (HDPE) and waste wood sawdust to prepare composites. Clearly a new science strategy was necessary for modification of the wood fibers, and we developed one by using colloidal sol–gel silica solution for introduction of silica particles within the fiber cell walls. The nanosilica, so introduced, was used as sites to attach micromolecules of 3-methacryloxypropyltrimethoxysilane (3MPS) coupling agents and to modify the hydrophilic character of the wood through formation of stable Si—O—Si bonds. These bonds are more hydrolytically stable than the cellulose equivalent C—O—Si bonds. Thus, the modified fibers should be more suitable for a polymer composite. Our aim was to improve the compatibility between HDPE matrix and wood sawdust and develop PWCs that have better properties than neat HDPE. For comparison, the blends of HDPE with 25.0 and 50.0 wt.% unmodified wood were also prepared and evaluated under identical conditions.

3. Experimental

3.1. Materials

Recycled wood sawdust samples were provided by Snider Industry as a gift. HDPE milk and water containers were collected randomly from several locations and were pelletized after cleaning. Tetraethyl orthosilicate (TEOS, $Si(OCH_3)_4$), 3-methacryloxypropyl-trimethoxysilane (3MPS, $H_2C{=}C(CH_3)CO_2(CH_2)_3Si(OCH_3)_3$), toluene ($C_7H_8$), and methanol ($CH_3OH$) were supplied by Aldrich Chemicals Co. Toluene and methanol were used as the solvents for the modification. All reagents were of analytical grade and were used as received.

3.2. Treatment of the wood

Two methods have been used to modify the wood surface:

Method 1: 3MPS coupling reagent was used to modify the hydrophilic character of the wood. The functional groups of the 3MPS are reacting with cellulose hydroxyls and forming C—O—Si silicate ester bonds. Grafted macromolecules are increasing the compatibility between polymer and fiber wall; however, it turned out that the C—O—Si covalent bonds between cellulose and silicon are insufficiently stable to have a strong and durable enhancement on wood fiber-polymer composite properties.

Experimental part: The reaction mixture contained 0.2 mol 3MPS, 1.9 mol toluene and 50 g wood. After dispersing the wood in solvent, we added 3MPS and refluxed the resulting mixture for 3 h during continuous mixing. Afterwards the fibers were washed with fresh solvent to remove the excess chemicals absorbed on the surfaces. Final products were dried at 70 °C under a vacuum for 24 h.

Method 2: We synthesized silica particles from Si-alkoxide using the traditional sol–gel process. So produced silica nanoparticles were embedded within the fiber cells in order to impart glass surface properties inside the wood. By embedding silica within the fiber cell wall and attaching a silane coupling agent—3MPS—to silanol groups, we tried to form a Si—O—Si bond between silicated fiber cells and 3MPS macromolecules.

Experimental part: Hydrolization and co-condensation of TEOS were conducted via a sol–gel reaction. A silica precursor (0.16 mol) in the presence of methanol (6.0 mol), deionized water (0.16 mol), and hydrochloric acid (0.001 mol) was mixed with 50.0 g wood at room temperature. After 3 h of mixing, we added 0.06 mol 3MPS and subjected the system to mixing 3 h more at 70 °C.

3.3. Sample preparation

Composites based on dried HDPE and wood particles were melted and mixed in a C.W. Brabender D-52 Preparation Station at the rotation speed of 80 rpm and at 135 °C. Composites obtained this way were pelletized and dried; they contained, in turn, 25.0 and 50.0 wt.% wood. Subsequently, the samples were molded in a Carver compression molding machine at 150 °C temperature and 2.07×10^4 kPa compression pressure. A total of six different materials were prepared.

3.4. Characterization techniques

Differential scanning calorimetry (DSC) and thermogravimetric analysis (TGA): DSC measurements were performed on a Perkin Elmer DSC-7 instrument. A sealed liquid-type aluminum capsule pan was used as a sample holder. The temperature range from 10 °C to 200 °C was covered under a nitrogen atmosphere at 10 °C/min heating rate. A Perkin Elmer TG-7 instrument was used to determine a temperature profile of the samples over the temperature range from 50 °C to 700 °C in nitrogen atmosphere at the heating rate of 10 °C/min. These techniques are clearly described by Menard [30]. Thermal analysis was performed on hot-pressed films.

Dynamic mechanical (DMA) and thermomechanical analysis (TMA): We performed these tests using a DMA7e apparatus from Perkin Elmer Co. Specimens were analyzed in rectangular form using the three point bending fixture in the temperature T scan mode. TMA experiments were performed over the temperature range from −50 °C to +100 °C at the heating rate of 10 °C/min with a compression analysis kit. TMA provides values of linear isobaric expansivity (often called thermal expansion coefficient or CTE) defined as

$$\alpha_L = L^{-1}(\partial L/\partial T)_P \tag{1}$$

L is the length (actually height, the distance between top and bottom parallel surfaces) of the sample, T = temperature, and P = pressure. These techniques are also described by Menard [30]. Volumetric isobaric expansivity $\alpha = V^{-1}(\partial V/\partial T)_P$, where V = volume, can be obtained from the determination of α_L. If the material is isotropic, one determination of α_L is sufficient. Otherwise three determinations along three Cartesian coordinates are needed.

Fourier-transform infrared spectroscopy (FTIR): The spectra were recorded on a Nexus 470 FTIR ESP Series spectrometer equipped with an attenuated total reflectance (ATR) objective. FTIR spectra were collected over the range from 4000 cm^{-1} to 650 cm^{-1} with the resolution of 4 cm^{-1}. To enhance the signal-to-noise ratio, each of the reference and sample spectra presented constitutes the average of 40 scans recorded.

Focused ion-beam + scanning electron microscopy (FIB/SEM): This combination of techniques has been reported as quite useful before [31]. The FEI Nova 200 NanoLab was used to study the morphology of the composites. A small fraction of the samples was mounted on a copper stub and coated with a thin layer of gold to avoid electrostatic charging during examination. A dual-beam FIB system is comprised of a high-resolution field emission SEM and scanning Ga^+ ion beam column. The composites were milled with a 0.5 nA Ga^+ ion beam current at an accelerating voltage of 30 kV. The inner region of the cross-section area was polished (cleaned) with a lower beam current 50 pA.

Tensile testing: The quasi-static tensile behavior of the samples was determined at room temperature with a MTS tester (model QTEST/5). The cross-head speed was 50 mm/min.

Dynamic friction testing: Friction tests were conducted on the Nanovea pin-on-disk tribometer from Micro Photonics reported before [29,32,33]; reviews of polymer tribology are available [34,35]. Each test was performed using 3.2 mm steel 302 balls (made by Salem Specialty Ball) under the following conditions: temperature 20 ± 2 °C, radius 2.0 mm, load 5 N, speed 100 rpm, and the number of revolutions with 3000 revolutions. Surface images of the samples and used balls were captured after friction tests using a Nicon Eclipse ME 600 microscope. Areas of wear tracks were measured with a Veeco Dektak 150 Profilometer. We used cross-sectional areas so obtained to estimate the wear volume V_m as

$$V_m = 2\pi R_m A_m \tag{2}$$

Here R_m and A_m represent the radius and the average cross-section area of wear track, respectively. The wear rate Z in mm^3/Nm was calculated as

$$Z = \frac{V_m}{WL} \tag{3}$$

Here V_m is the volume loss of the sample after testing, W is the normal load, L is the length.

Scratch resistance: Micro-Scratch Tester (MST) from Anton Paar was used. For each sample, progressive scratch and multiple scratch testing were performed. The parameters for progressive scratch were: initial load 1.0 N, final load 30.0 N, loading rate 10.0 N/min, scanning load 0.05 N, scratch length 5.0 mm and scratch speed 5.9 mm/min. The conical diamond intender had a diameter of 200 μm and a cone angle of 120°. One so determines the instantaneous or penetration depth R_p and the residual or healing depth R_h (2 min after the scratch run). This technique has been also explained in reviews on polymer tribology [34,35].

4. Characterization of Modified Wood Sawdust by EDS and TGA

To determine the progress of the modification process, we analyzed ashes remaining after burning the wood samples at 700 °C. Energy dispersive spectroscopy (EDS) shows significant difference between the samples. EDS spectra of the wood ash before treatment gave only the peaks of microelements corresponding to contaminations – impurities of the wood "sawdust" (Fig. 1a).

Strong Si—, and O— peaks in modified wood samples are the evidence of the modification progress. EDS of the modified wood did not detect microelements due to extraction from the wood during high temperature treatment and purification.

Thermogravimetric analysis (TGA) has been performed to obtain more evidence elucidating the progress of the modification process. The amount of the residuals increased from 0.6 to 6.8 and 20.4 wt.%, respectively, upon modification. The differences can be assigned to the inorganic part of the modified wood that survived after heating the samples at 700 °C. The organic part inside wood all decomposed below 500 °C. Significant differences between residuals of the unmodified and modified sample are associated with the modification process.

Another beneficial effect of modification is the increase in hydrophobicity. TGA results (Fig. 2a) clearly suggest that the obtained network is highly hydrophobic and confers moisture resistance to the hybrids.

Wood modification reaction with 3MPS was followed up by Fourier transform infrared spectroscopy (FTIR) (Fig. 2b). The presence of Si—O—$C_{cellulose}$, Si—O—Si bonds, and the carbonyl stretching band —C=O at ca. 1716 cm^{-1} on the cellulose surface confirms that the silane coupling agent 3MPS was efficiently held on the fibers surfaces through both condensation with cellulose hydroxyl groups and self-condensation between silanol groups. The bends at 550 cm^{-1} and 817 cm^{-1} are related to the symmetric bending and stretching vibrations of inter-tetrahedral oxygen atoms present in silica (symmetric Si—O—Si stretching), while the peak at 1156 cm^{-1} represents characteristic Si—O—C cellulose vibrations.

FTIR spectra (Fig. 2b) of wood/sol–gel silica sample are nearly identical to wood/3MPS spectra. In Method 2 the band intensity for Si—O—Si at 555 cm^{-1} and 813 cm^{-1} became more pronounced and the band intensity for Si—O—$C_{cellulose}$ at 1160 cm^{-1} slightly decreased. TGA data, together with EDS and FTIR, gave us evidence of successful wood modification process.

Moreover, during SEM and EDS examination of the wood ashes, we noticed completely different morphologies for each wood samples. We recall that all three wood samples were heated at 700 °C for 1 h. For sol–gel silica modified wood samples, we noticed many scattered rods (Fig. 3c).

We decided to investigate the rods further. The results turned out to be fairly impressive. We increased heat treatment time from 1 to 2 and 3 h respectively, to evaluate better the effect of the heat treatment at 700 °C (see Fig. 4).

The longer we burned the wood, the more evident the rod structures became. EDS data further revealed that these rods are in fact silica rods (Fig. 5).

FTIR data show a broad band around 1045.6 cm^{-1}, the characteristic peak of the anti-symmetric stretching vibrational mode of the Si—O—Si siloxane bridges. The other two bands detected at about 796.4 cm^{-1} and 444.9 cm^{-1} are also assigned to Si—O—Si siloxane bridges. The peak at 796.4 cm^{-1} is related to the symmetric vibration mode of the Si—O—Si bridges, and the 444.9 cm^{-1} peak corresponds to the vibrational adsorption peak of the Si—O—Si siloxane bridges, which is the characteristic peak of silica. The clean FTIR spectrum also indicates that there are no other impurities adsorbed onto the surface of the silica rods. In order to understand formation of the rods, we also examined the ash sample of the sol–gel treated wood after heating one at 700 °C only for 5 min (Fig. 6).

As we know, wood consists mainly of two kinds of cells: *wood fibers and vessel elements*. Wood fibers are elongated cells, which are similar to tracheids but smaller, only 0.7 mm to 3 mm long and less than 20×10^{-6} m in diameter. SEM image shows us that silica nanoparticles are filling wood-fiber cells. In a later stage, namely during high temperature heating, so introduced particles bonded with each other and created a strong silica network. In this process, silica-functionalized wood fiber cells act as a structure-determining "agent." This observation once again proves that wood sawdust was successfully modified using sol–gel approach in combination with 3MPS (Method 2).

5. Thermal properties determined by DSC

As discussed by Menard [30] thermal characterization of the crystalline or semi-crystalline polymers provides us information about melting temperature T_m, crystallization temperature T_c, and enthalpy of fusion H^f in Jg^{-1}. Melting and crystallization parameters are displayed in Table 1.

From DSC thermograms relatively sharper and stronger melting peaks are observed for recycled HDPE (R-HDPE), indicating the decrease of fusion enthalpy and the presence of less homogeneous crystalline structures in the composites. The melting (T_m) and crystallization (T_c) temperatures of R-HDPE are slightly influenced by wood fibers. For example, T_m decreases from 130 °C of R-HDPE to 129 °C and 127 °C of composites containing 25.0 and 50.0 wt.% neat wood, respectively. Thus, the crystalline lamella thickness of R-HDPE in composites is smaller than that in neat R-HDPE. The fusion enthalpy and crystallization of R-HDPE were found to be 184 Jg^{-1} and 63%, respectively. From DSC curves one can see that the crystallization peak temperatures (T_c) of composites are slightly altered; significantly narrow and weak intensity of the melting and crystallization signals suggests a progressive decrease in the overall crystallization upon

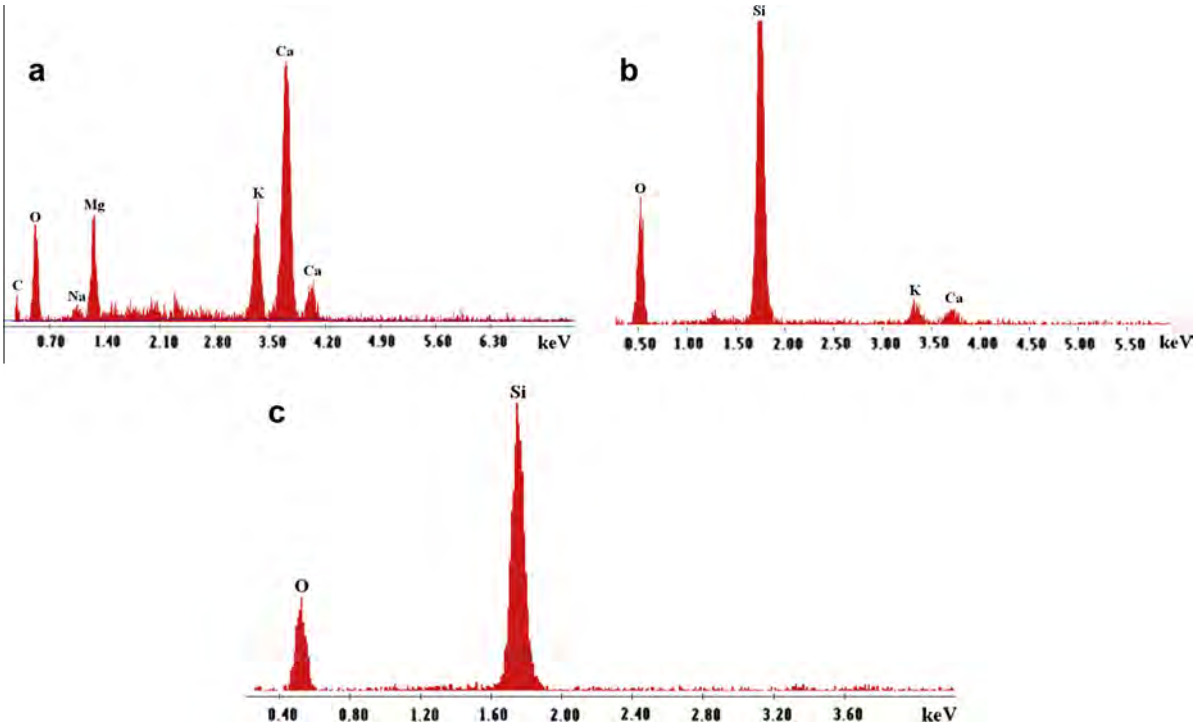

Fig. 1. EDS of the wood ashes: neat wood (a); wood/3MPS (b); wood/sol–gel modified (c).

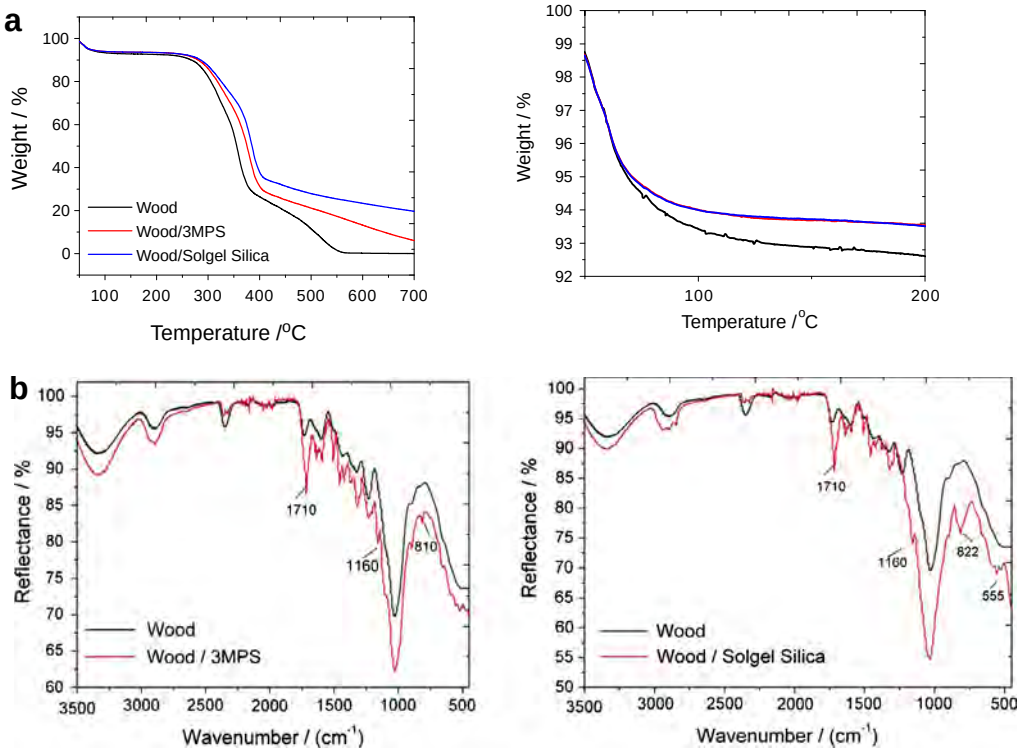

Fig. 2. TGA (a) and FTIR (b) diagrams of the neat and modified wood.

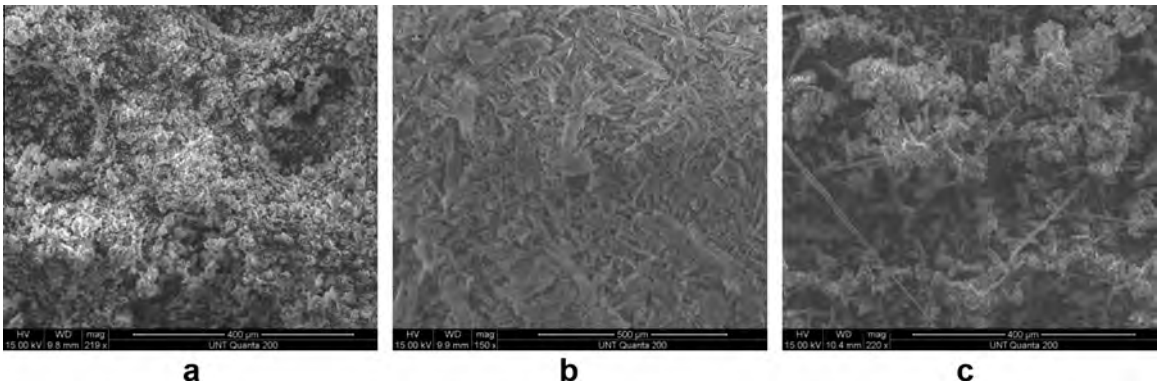

Fig. 3. ESEM images: wood ash (a), wood/3MPS ash (b) and wood/sol–gel silica ash (c).

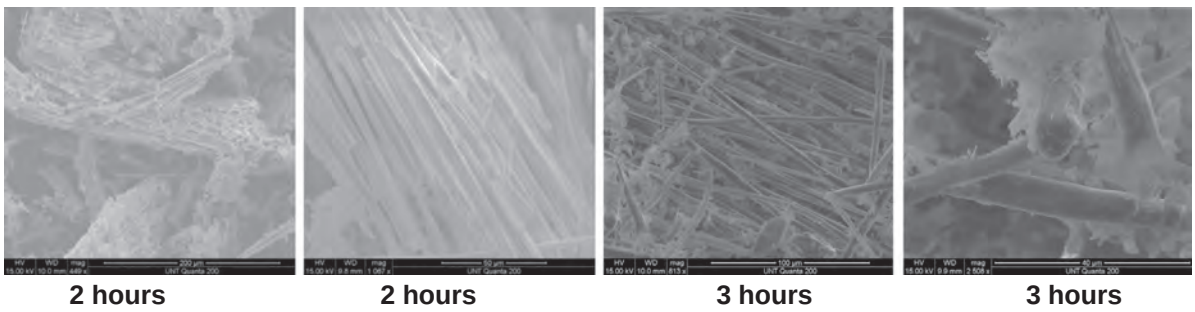

Fig. 4. ESEM images: wood/sol–gel silica ash.

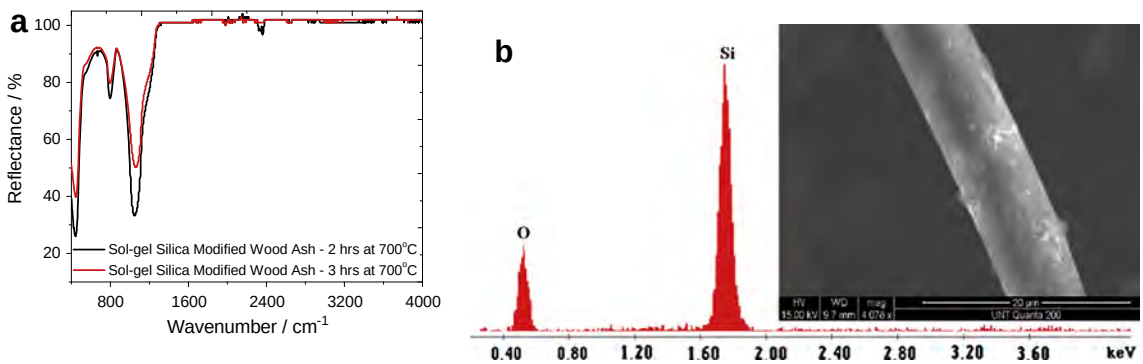

Fig. 5. FTIR (a) of the wood/sol–gel modified ash and a SEM/EDS (b) of the single rod.

fiber loading. As expected, the presence of wood lowers the degree of crystallinity of R-HDPE. There is a decrease of crystallinity from 63% to 18% after filling the matrix with 50.0 wt.% wood. However, applying 3MPS treatment increases the crystallinity to 28% while the sol–gel approach together with 3MPS application results in crystallinity equal to 32%.

Similar but necessarily smaller effects are seen for 25.0 wt.% wood composites. Inclusion of unmodified wood lowers the degree of crystallinity from 63% to 46%. Treatment with 3MPS increases the crystallinity to 49%, treatment with a combination of sol–gel technique plus 3MPS to 50%.

The fact that the composites have lower crystallinities than neat R-HDPE is easily understandable. Interesting is the fact that modification of the fibers *enhances* crystallinity. Below in Section 8 we report that the fibers *after modification* are covered with R-HDPE. Thus, fiber surfaces can now serve as nucleation sites for crystallization.

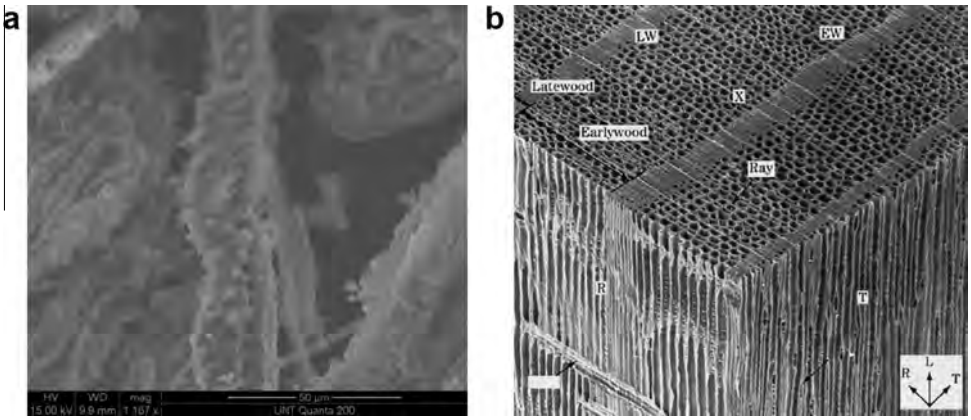

Fig. 6. ESEM images: wood/sol–gel silica ash/5 min at 700 °C and wood microstructure [23].

Table 1
Melting and crystallization parameters.

Materials	T_c/°C	T_m/°C	ΔH/Jg^{-1}	X_c/%
R-HDPE	102	130	184	63
R-HDPE + 25 wt.% wood	101	129	136	46
R-HDPE + 50 wt.% wood	105	127	54	18
R-HDPE + 25 wt.% wood/3MPS	103	132	145	49
R-HDPE + 50 wt.% wood/3MPS	100	132	82	28
R-HDPE + 25 wt.% wood/sol–gel silica	102	129	146	50
R-HDPE + 50 wt.% wood/sol–gel silica	102	129	94	32

6. Mechanical properties and thermal expansivity

Mechanical properties of wood + R-HDPE composites were evaluated using DMA, and tensile testing while TMA was used to determine thermal expansivity. Influence of the temperature on the mechanical response of the materials was studied by DMA. The storage modulus E' and the tan delta as a function of the temperature are shown in Fig. 7a. Linear isobaric expansivity values (see Eq. (1)) are displayed in Fig. 7b, including error bars.

We see that the storage modulus E' increased after wood addition to R-HDPE. Higher E' is seen for all samples, but the improvement is higher for modified composites. The highest E' were obtained for R-HDPE + wood/MPS samples, relatively low E' values for composites with unmodified wood. One can conclude from DMA data that wood fibers became stiffer after modification. Tan delta curves presented above show α-relaxation in the −130 °C to −100 °C temperature range and can be used to locate the glass transition region and the glass transition temperature T_g. That temperature reflects significantly long range motions of the main chains. Compared to neat R-HDPE, the tan δ peak of the composites slightly shifts to higher temperatures, but there are no significant differences between the T_g values of the composites. Furthermore, the higher temperature relaxation, known as β-relaxation was observed for the composites in the temperature range −45 °C to −55 °C temperature; the appearance of the peak becomes noticeable upon increased wood content. We see here conformational changes experienced in the cellulose or hemicellulose fragments of the wood.

We have determined thermal expansivity (TE) of our composites; see again Eq. (1) above. The dimensional changes of the samples were measured in the temperature range −50 °C to +50 °C. The values of TE at 25 °C are presented in Fig. 8b. We see that TE decreases with the increase of the wood content. Expansivity of R-HDPE is $9.82 \cdot 10^{-5}$/°C while for R-HDPE + 25 wt.% wood and for R-HDPE + 50.0 wt.% wood the values are $9.25 \cdot 10^{-5}$/°C and $7.70 \cdot 10^{-5}$/°C, respectively. Thermal expansion also involves the transmission of stress across an interface, and should thus throw light on the adhesion between the phases. R-HDPE + wood composites form two-phase systems; their expansion is higher than that of composites prepared with surface-modified wood particles. This phenomenon might be related to interface adhesion. When one heats unmodified composites, the matrix expansion is more than that of the fillers. Because of poor adhesion between the two phases, there are no residual compressive stresses across the interface. As a result, the matrix expands away from the fibers. Considering all composites, the sol–gel silica modified samples have the lowest TE while unmodified wood-filled samples have the highest TE. Recall that the sol–gel modified wood composites contain inorganic silica particles. As we know, the intrinsic TE of silica is lower than TEs of wood or HDPE. As a result, well dispersed silica filler plays a significant role in the dimensional stability of our composites.

The tensile properties of the composites as well as of neat R-HDPE were determined. We present the Young modulus and the strain at break results in Fig. 8, including error bars.

Young modulus E values for the blends filled with wood are about 1.2 times higher than for neat R-HDPE. The increase in the modulus with fiber loading shows the same linear trend as observed for the thermal expansivity. Higher modulus E

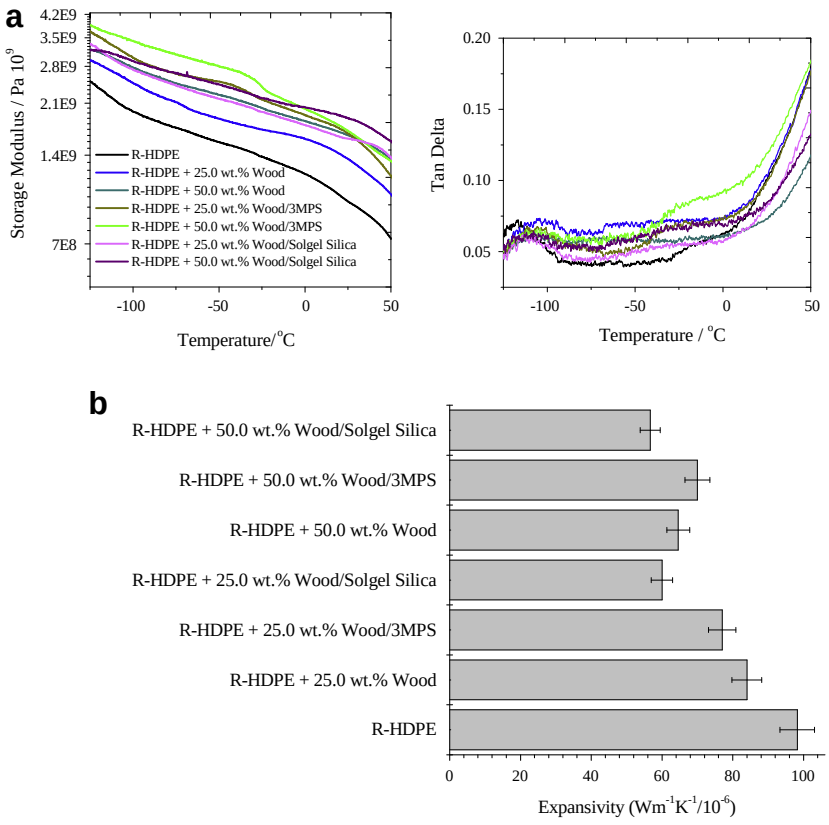

Fig. 7. DMA (a) and TMA diagrams (b).

values are seen for all the composites. However, E values did not show significant change and remained almost constant after treatment with 3MPS (as compared to the samples with unmodified wood). The most effective treatment was found to be sol–gel process (Method 2). The samples prepared via this method display the highest modulus. Moreover, for any given fiber loading, sol–gel modified wood samples had the highest modulus increment, equal to 512 MPa. One can clearly see that the sol–gel process induced the enhancement of tensile strength from 1361 MPa of neat R-HDPE to 3313 MPa of R-HDPE + 50.0 wt.% wood composite. The results can be attributed to the presence of the silica particles when compared to other composites. Another possible reason to explain the higher modulus of sol–gel modified wood composites is improved adhesion between the wood and polymer interfaces.

Values for the strain at break of our composites are presented also in Fig. 8. The strain at break ϵ_b of all samples decreases with increasing amount of the wood fibers. We recall that the material brittleness [36] is inversely proportional to ϵ_b:

$$B = 1/(E'\epsilon_b) \tag{4}$$

The E' values at room temperature are those from DMA results in three point bending. Fig. 8 shows that the strain at break of the composites had fallen rapidly from 3.8% to 0.8% upon loading the matrix with 25.0 wt.% and 50.0 wt.% wood fibers, respectively. The descent of ϵ_b is faster than the increase in E'. Therefore, the brittleness values increase from $1.44 \cdot (10^{-10}\%\ \text{Pa})$ of R-HDPE to $7.97 \cdot (10^{-10}\%\ \text{Pa})$ for the composite with 50.0 wt.% wood content. All these values are small. Polystyrene, admittedly a very brittle polymer, has $B = 878 \cdot (10^{-10}\%\ \text{Pa})$ [36,37]. We note that B is inversely proportional to tensile toughness [38].

Addition of the surface modified wood did not affect tensile behavior significantly. The treatment, however, produced lower values of the brittleness as well as higher percent of the strain at break as compared to unmodified samples. Thus, modification also helps for enhancing the elongation at break and lowering brittleness.

7. Tribological properties

Friction, wear and scratch resistance results also contribute to the conclusion that the modified wood samples have better strength and higher load-carrying capacity than the unmodified samples or the neat R-HDPE. In scratch resistance testing, all wood composites have lower penetration and residual depths compared to neat HDPE (Fig. 9).

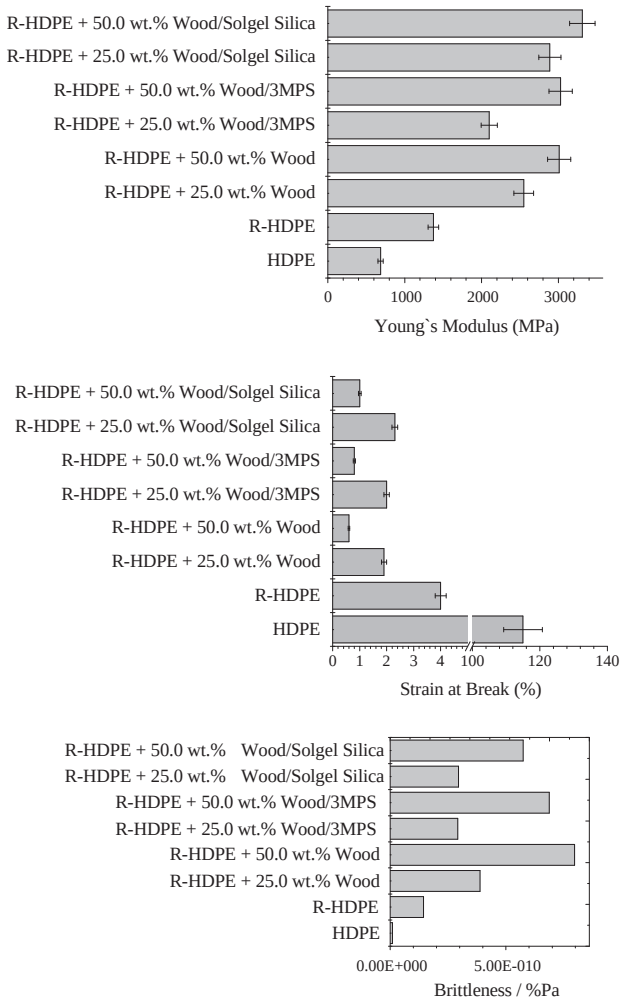

Fig. 8. Tensile properties and brittleness.

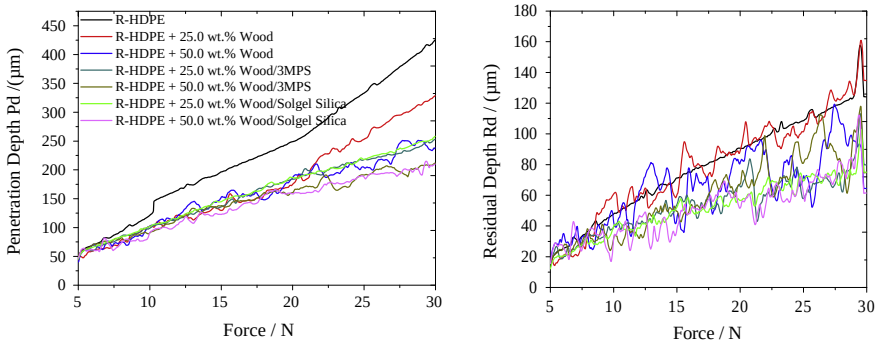

Fig. 9. Progressive scratch testing results.

The modified samples were more stable to instantaneous deformations at loads higher than 20.0 N. Overall, high scratch resistance was found for R-HDPE + 50.0 wt.% wood/sol–gel silica and R-HDPE + 50.0 wt.% wood/3MPS samples. This applies to both penetration and residual depth. Neat-wood-containing polymer composites show less viscoelastic recovery, while the samples with modified wood gave lower value of the residual depth. However, wood content did not show significant effect on the materials viscoelastic recovery. The recovery percentage is defined as $f = (R_p - R_h)\cdot 100\%/R_p$.

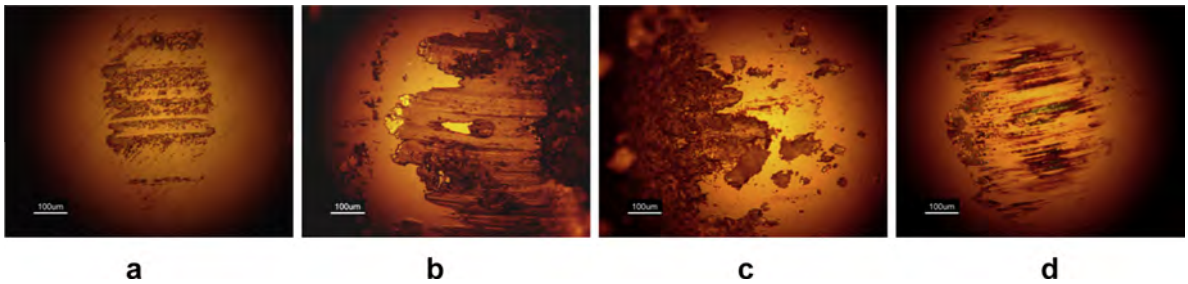

Fig. 10. Optical microscopy images of the HDPE (a) and composites with: 50.0 wt.% wood (b), 50.0 wt.% wood/3MPS (c), 50.0 wt.% wood/sol–gel silica (d).

Optical observation of the ball surfaces after dynamic friction test revealed the film transfer phenomenon (Fig. 10).

Tribological (friction and wear) data support our assumption about the film formation process. This is directly associated with the poor adhesion between the wood and polymer interfaces. The lowest friction was observed in the neat polymer while the highest was observed in the HDPE + wood sample. All the composites rapidly reached the steady friction value in an early stage of the test. Friction increased slightly upon applying the higher load. Tribology data did not provide us correlation between friction and the test conditions; however, in all cases the friction of the samples with modified wood showed the lowest friction compared to composites containing the same but neat wood.

Optical observations of the ball surface aimed at explaining tribological response of the composites. Compared to sol–gel modified wood composites (Fig. 10d), more film transfer was noticed for neat wood and wood/3MPS containing samples. Surface area increases due to film transfer and so does friction.

8. Morphology

We conducted microscopic examinations to explain mechanical and tribological response and to study the role of surface treatment on the deformation processes of our composites. FIB/SEM images of the various composites with 50.0 wt.% wood content are presented in Fig. 11. Parallelepipeds were cut out by FIB milling before SEM observations.

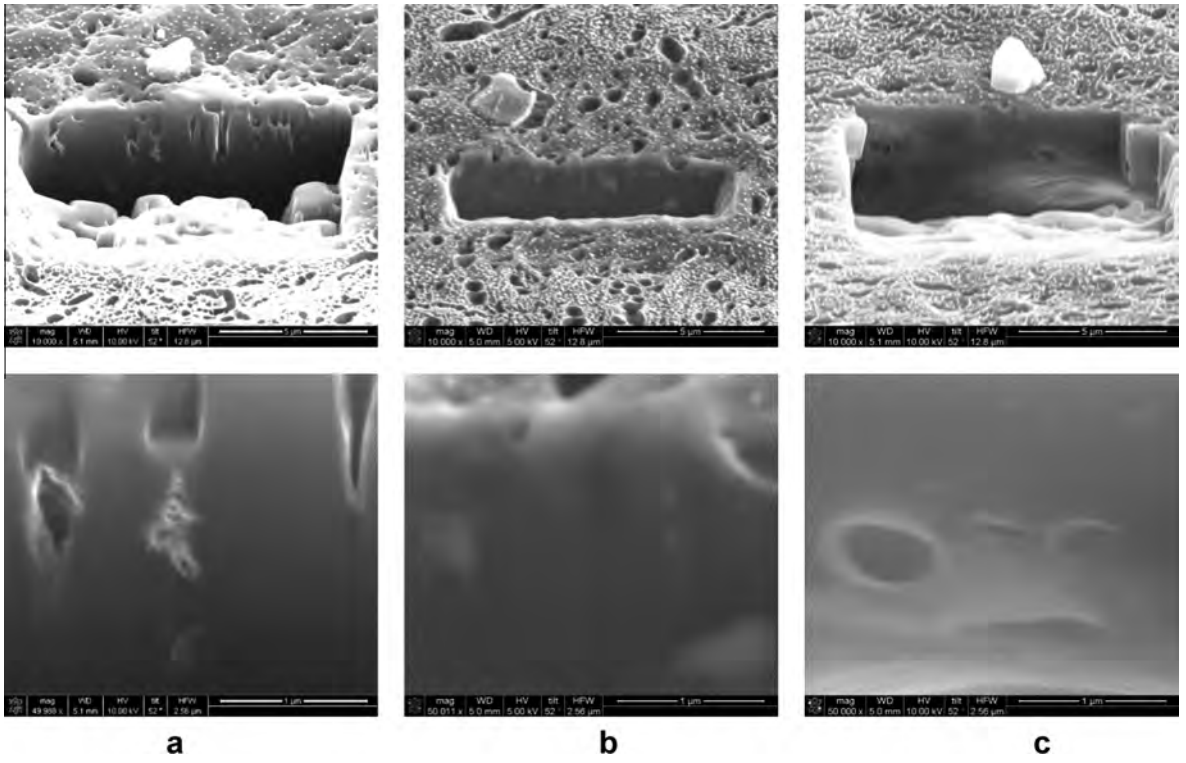

Fig. 11. FIB/SEM images of the HDPE composites with: 50.0 wt.% wood (a), 50.0 wt.% wood/3MPS (b), 50.0 wt.% wood/sol–gel silica (c).

Improvement in interfacial adhesion upon wood surface modification is apparent from FIB/SEM micrographs. Morphology of the composites became more uniform when modifiers are added into the system. A sample with neat wood (Fig. 11a) does not show evidence of adhesion between the fibers and the polymer matrix; gap between the two phases as well as empty domains are clearly noticeable in high magnification images. An examination of the composites filled with 50.0 wt. % modified wood (Fig. 11b and c) reveals that fibers seem to be covered with R-HDPE. This fact may be explained by a stronger interaction between the two phases, resulting in higher adhesion between the components. The morphological observations are consistent with the mechanical and tribological performance of the composites.

Overall, the sol–gel modification process, that is Method 2, obviously had positive effects on the bond and strength of the R-LDPE + wood sawdust materials. While the importance of natural fibers is increasing [39–41], methods of providing their strong adhesion to polymeric matrices is becoming more important as well.

For generality, we note that our approach of using wood sawdust is only one option of using materials available in Nature [42]. Bamboo is a material used in housing construction in several countries. The problem in combining bamboo with polymers is similar to ours: lack of good interfacial adhesion. Guimarães et al. [43] used NaOH and benzophenone tetracarboxylic dianhydride to improve the adhesion – with good results. Also water absorption was lowered significantly.

Acknowledgments

Research scholarships awarded to two of us (P.J. and H.M.) by the Texas Academy of Mathematics and Science, Denton, are gratefully acknowledged.

References

[1] J.E. Winandy, N.M. Stark, C.M. Celmons, in: Proceedings of the 5th Global Wood and Natural Fibre Composites Symposium. Kassel, ED# A6-1-A69, 2004.
[2] Anon, Editorial on "Demand for wood and agriculture fibers", BRIEF-reinforced Plastics 24 (2000) 1–2.
[3] S.L. Moore, D. Gregorio, M. Carreon, S.B. Weisberg, M.K. Leecaster, Composition and distribution of beach debris in Orange County, California, Mar. Pollut. Bull. 42 (2001) 241–245.
[4] C.J. Moore, S.L. Moore, M.K. Leecaster, S.B. Weisberg, A comparison of plastic and plankton in the North Pacific central gyre, Mar. Pollut. Bull. 42 (2001) 1297–1300.
[5] R.C. Thompson, Y. Olsen, R.P. Mitchell, A. Davis, S.J. Rowland, A.W.G. John, D. McGonigle, A.E. Russell, Lost at sea: where is all the plastic?, Science 304 (2004) 838
[6] J.P. Barreiros, J. Barcelos, Plastic ingestion by a leatherback turtle Dermochelys coriacea from the Azores (NE Atlantic), Mar. Pollut. Bull. 42 (2001) 1196–1197.
[7] L. Bugoni, L. Krause, M.V. Petry, Marine debris and human impacts on sea turtles in southern Brazil, Mar. Pollut. Bull. 42 (2001) 1330–1334.
[8] J. Tomas, R. Guitart, R. Mateo, J.A. Raga, Marine debris ingestion in loggerhead sea turtles *Caretta caretta* from the Western Mediterranean, Mar. Pollut. Bull. 44 (2002) 211–216.
[9] S.K. Najafi, E. Hamidinia, M. Tajvidi, Mechanical properties of composites from sawdust and recycled plastics, J. Appl. Polym. Sci. 100 (2006) 3641–3645.
[10] J. Balatinecz, M. Sain, The influence of recycling on the properties of wood fibre-plastic composites, Macromol. Symp. 135 (1998) 167–173.
[11] Y. Cui, S. Lee, B. Noruziaan, M. Cheung, J. Tao, Fabrication and interfacial modification of wood/recycled plastic composite materials, Compos. Part A 39 (2008) 655–661.
[12] J. George, M. Sreekala, S. Thomas, A review on interface modification and characterization of natural fiber reinforced plastic composites, Polym. Eng. Sci. 41 (2001) 1471–1485.
[13] P. Razi, R. Portier, A. Raman, Studies on polymer-wood interface bonding: effect of coupling agents and surface modification, J. Compos. Mater. 33 (1999) 1064–1079.
[14] K. Jayaraman, D. Bhattacharyya, Mechanical performance of wood fiber-waste plastic composite materials, Resour. Conserv. Recycl. 41 (2004) 307–319.
[15] M. Fossen, G. Ormel, G. VanVilsteren, T. Jongsma, Lignocellulosic fibre reinforced caseinate plastics, Appl. Compos. Mater. 7 (2000) 433–437.
[16] A. Bledzki, J. Gassan, Composites reinforced with cellulose based fibres, Prog. Polym. Sci. 24 (1999) 221–274.
[17] K. Van De Velde, P. Kiekens, Influence of fiber surface characteristics on the flax/polypropylene interface, J. Thermopl. Compos. Mater. 14 (2001) 244–260.
[18] M. Narkis, J.H. Chen, Review of methods for characterization of interfacial fiber–matrix interactions, Polym. Compos. 9 (1988) 245–251.
[19] L.A. Pothan, S. Thomas, G. Groeninckx, The role of fibre/matrix interactions on the dynamic mechanical properties of chemically modified banana fibre/polyester composites, Compos. Part A – Appl. Sci. 37 (2006) 1260–1269.
[20] A. Kopczynska, G.W. Ehrenstein, Polymeric surfaces and their true surface tension in solids and melts, J. Mater. Ed. 29 (2007) 325–340.
[21] R.C. Desai, R. Kapral, Dynamics of Self-organized and Self-assembled Structures, Cambridge University Press, Cambridge – New York, 2009.
[22] G.H. Michler, F.J. Balta-Calleja, Nano- and Micromechanics of Polymers: Structure Modification and Improvement of Properties, Hanser, Munich – Cincinnati, 2012.
[23] P. Koch, Utilization of the Southern Pines, The Raw Material, USDA Forest Service, Agricultural Handbook, 420 (1972) 733.
[24] K.Y. Lee, M. Tang, C.K. Williams, A. Bismarck, Carbohydrate derived copoly(lactide) as the compatibilizer for bacterial cellulose reinforced polylactide nanocomposites, Compos. Sci. Technol. 72 (14) (2012) 1646–1650.
[25] K.L. Pickering, A. Abdalla, C. Ji, A.G. McDonald, R.A. Franich, The effect of silane coupling agents on radiata pine fibre for use in thermoplastic matrix composites, Compos. Part A 34 (2003) 915–926.
[26] M. Bengtsson, K. Oksman, The use of silane technology in crosslinking polyethylene/wood flour composites, Compos. Part A – Appl. Sci. 37 (2006) 752–765.
[27] Y. Xie, C.A.S. Hill, Z. Xiao, H. Militz, C. Mai, Silane coupling agents used for natural fiber/polymer composites: a review, Compos. Part A 41 (2010) 806–819.
[28] J. Felix, P. Gatenholm, The nature of adhesion in composites of modified cellulose fibers and polypropylene, J. Appl. Polym. Sci. 42 (1991) 609–620.
[29] W. Brostow, W. Chonkaew, T. Datashvili, K.P. Menard, Tribological properties of epoxy + silica hybrid materials, J. Nanosci. Nanotech. 9 (2009) 1916–1922.
[30] K.P. Menard, in: W. Brostow (Ed.), Performance of Plastics, Hanser – Gardner, Munich – Cincinnati, 2000.
[31] W. Brostow, B.P. Gorman, O. Olea-Mejia, Focus ion beam milling and scanning electron microscopy characterization of metal + polymer hybrids, Mater. Lett. 61 (2007) 1333–1336.

[32] W. Brostow, W. Chonkaew, K.P. Menard, T. Scharf, Modification of an epoxy resin with a fluoroepoxy oligomer for improved mechanical and tribological properties, Mater. Sci. Eng. A 507 (2009) 241–251.
[33] V.H. Orozco, W. Brostow, W. Chonkaew, B. Lopez, Preparation and characterization of poly (lactic acid)-g-maleic anhydride + starch blends, Macromol. Symp. 277 (2009) 69–80.
[34] W. Brostow, J.-L. Deborde, M. Jaklewicz, P. Olszynski, Tribology with emphasis on polymers: friction, scratch resistance and wear, J. Mater. Ed. 25 (2003) 119–132.
[35] W. Brostow, V. Kovacevic, D. Vrsaljko, J. Whitworth, Tribology of polymers and polymer based composites, J. Mater. Ed. 32l (2010) 273–290.
[36] W. Brostow, H.E. Hagg Lobland, M. Narkis, Sliding wear, viscoelasticity, and brittleness of polymers, J. Mater. Res. 21 (2006) 2422–2428.
[37] W. Brostow, H.E. Hagg Lobland, M. Narkis, The concept of materials brittleness and its applications, Polym. Bull. 59 (2011) 1697–1707.
[38] W. Brostow, H.E. Hagg Lobland, S. Khoja, Mater. Lett. 159 (2015) 478–480.
[39] F.R. Cichocki, J.L. Thomason, Thermoelastic anisotropy of a natural fiber, Compos. Sci. Technol. 62 (5) (2002) 669–678.
[40] L. Suryanegara, A.N. Nakagaito, H. Yano, The effect of crystallization of PLA on the thermal and mechanical properties of microfibrillated cellulose-reinforced PLA composites, Compos. Sci. Technol. 69 (7–8) (2009) 1187–1192.
[41] N. Soykeabkaew, N. Laosat, A. Ngaokla, N. Yodsuwan, T. Tunkasiri, Reinforcing potential of micro- and nano-sized fibers in the starch-based biocomposites, Compos. Sci. Technol. 72 (7) (2012) 845–852.
[42] W. Brostow, T. Datashvili, H. Miller, Wood and wood derived materials, J. Mater. Ed. 32 (2010) 125–138.
[43] M. Guimarães Jr., K.M. Novack, V.R. Botaro, Bamboo pulp treated with NaOH and benzophenone tetracarboxylic dianhydride as reinforcement of new polymeric materials, Rev. LatinAm. Metal. Mater. 34 (2014) 196–208.